nature COMMUNICATIONS

ARTICLE

Received 31 May 2015 | Accepted 23 Mar 2016 | Published 6 May 2016

DOI: 10.1038/ncomms11413 OPEN

Perspective on the phase diagram of cuprate high-temperature superconductors

Damian Rybicki[1,2], Michael Jurkutat[1], Steven Reichardt[1], Czesław Kapusta[2] & Jürgen Haase[1]

Universal scaling laws can guide the understanding of new phenomena, and for cuprate high-temperature superconductivity the influential Uemura relation showed, early on, that the maximum critical temperature of superconductivity correlates with the density of the superfluid measured at low temperatures. Here we show that the charge content of the bonding orbitals of copper and oxygen in the ubiquitous CuO_2 plane, measured with nuclear magnetic resonance, reproduces this scaling. The charge transfer of the nominal copper hole to planar oxygen sets the maximum critical temperature. A three-dimensional phase diagram in terms of the charge content at copper as well as oxygen is introduced, which has the different cuprate families sorted with respect to their maximum critical temperature. We suggest that the critical temperature could be raised substantially if one were able to synthesize materials that lead to an increased planar oxygen hole content at the expense of that of planar copper.

[1] Institute of Experimental Physics II, University of Leipzig, Faculty of Physics and Earth Sciences, Linnéstrasse 5, Leipzig 04103, Germany. [2] AGH University of Science and Technology, Faculty of Physics and Applied Computer Science, Department of Solid State Physics, al. A. Mickiewicza 30, Krakow 30-059, Poland. Correspondence and requests for materials should be addressed to D.R. (email: ryba@agh.edu.pl).

The understanding of the complex properties of the cuprates, and what causes their high critical temperature of superconductivity (T_c), is one of the greatest challenges in condensed matter physics. From it one expects clues that make the synthesis of cuprates with much higher T_c possible or of how to improve other fundamental properties. In particular, it is still not well understood what sets the very different, maximum T_c's for different families of materials. An early experimental observation in this regard is the famous Uemura plot[1]. It shows that the maximum T_c is correlated with the muon spin relaxation rate σ_0 (extrapolated to $T=0$ K) that is proportional to the superfluid density divided by the effective mass ($\sigma_0 \propto n_s/m^*$). This relation holds for the underdoped materials and orders different cuprate families with respect to their maximum T_c. The Uemura relation and subsequent scaling laws have remained stimulating, up to now, and some were shown to be valid for other superconductors as well[2–9]. While there are various attempts at a theoretical explanation of the Uemura relation[4,10–12], a connection to other experimentally probed properties of cuprates is still lacking, in particular to material chemistry parameters.

The various cuprate families have in common, see Fig. 1a, a CuO_2 plane and charge reservoir (CR) layers that separate the planes from each other. While the nearly square CuO_2 plane, defined by the Cu $3d_{x^2-y^2}$ orbital bonding to four O $2p_\sigma$ orbitals, is very similar for all systems, the CR chemistry can vary significantly. The nominal hole at Cu ($3d^9$ configuration) is responsible for strong magnetic correlations that make parent materials antiferromagnetic. Holes or electrons can be added to the CuO_2 plane by alteration of CR layers. As a result, static magnetism vanishes and new electronic phenomena emerge and the systems become conducting or superconducting. There are many similarities between different cuprate families, and one typically differentiates only between the hole and electron-doped phase diagrams, depicted in Fig. 1b, that appear to show a distinct asymmetry. However, the extent in temperature and doping of the different phases and observed phenomena varies substantially between different families, also for the much more thoroughly investigated hole doped materials. In addition, the comparability between different families is somewhat obstructed with regard to doping. For example, while for $La_{2-x}Sr_xCuO_4$ the doping level can be varied over a large range quite reliably by stoichiometry, interstitial doping with oxygen (O_δ) as, for example, in $HgBa_2CuO_{4+\delta}$ leaves uncertainties with regard to the actual doping level. In addition, ionic migration may cause phase separation or other ordering phenomena as in the $YBa_2Cu_3O_{6+y}$ systems. Given the very different T_c for various cuprate families, it was questioned whether the average doping level of the CuO_2 plane is the appropriate chemical parameter for discussing all aspects of the complex physical properties of the cuprates, or whether other parameters should be considered as well, for example, distances within the plane, buckling, disorder, the role of the apical oxygen, or interlayer coupling. Nevertheless, from the understanding of the electronic properties we expect, in particular, clues as how to raise T_c.

Nuclear magnetic resonance (NMR), as a local probe of the magnetic spin susceptibility, focusses mostly on measurements of shift and relaxation caused by the interaction of the nuclear magnetic dipole moment with electronic magnetic moments. However, the nuclear electric quadrupole moment for nuclei with spin $I>1/2$ ($I=3/2$ for ^{63,65}Cu, $I=5/2$ for ^{17}O) interacts with the local electric field gradient (EFG) causing a quadrupole splitting (ν_Q) of the NMR lines in high magnetic fields. The EFG at the nuclear site is very sensitive to the local charge symmetry, and has been useful for assigning NMR signals to the various lattice positions or detecting inhomogeneous charge distributions in the CuO_2 plane[13,14]. Since the quadrupole splittings of planar Cu and O depend on doping, models have been put forward that attempted to understand these changes in terms of the hole content of certain orbitals, see for example, refs 15–18 and works

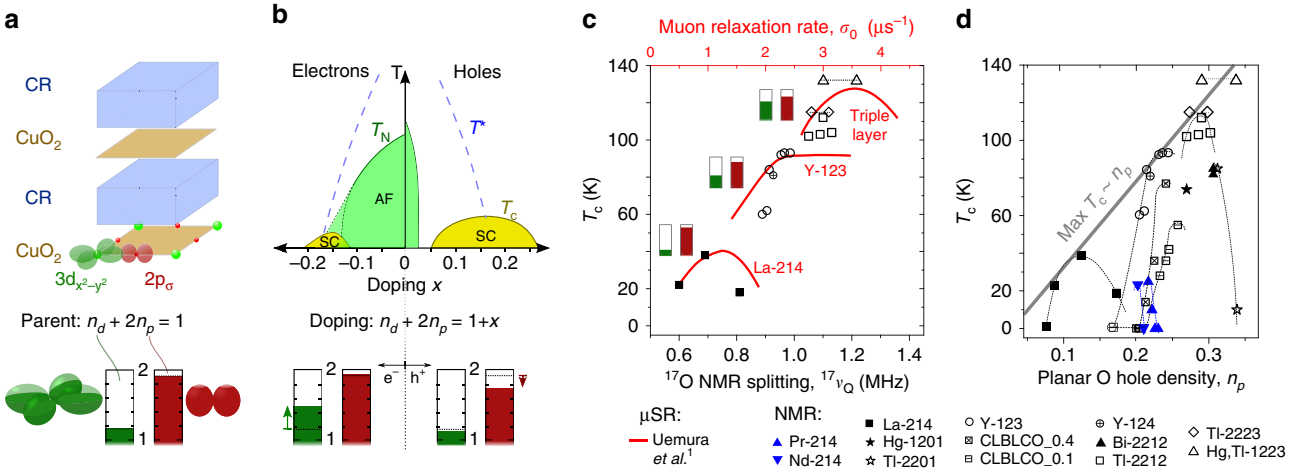

Figure 1 | General features of the cuprates. (**a**) The cuprates' layered structure consists of CR layers and CuO_2 planes with the bonding orbitals Cu $3d_{x^2-y^2}$ and O $2p_\sigma$, which share the nominal $3d$ hole of the Cu^{2+} ion. Columns indicate occupation of Cu $3d_{x^2-y^2}$ ($2-n_d$) and O $2p_\sigma$ ($2-n_p$), with hole contents n_d and n_p measurable with NMR. (**b**) Schematic representation of electronic phase diagram of the cuprates for electron and hole doping x: AF phase below Néel temperature (T_N), SC below critical temperature (T_c), and pseudogap regime below pseudogap temperature (T^*). Doped electrons (e^-) go to the Cu $3d_{x^2-y^2}$ orbital almost exclusively, while doped holes (h^+) predominantly go to the O $2p_\sigma$ orbital, arrows next to columns indicate changes of n_d and n_p caused by doping. (**c**) Solid red: Uemura plot[1], that is, T_c versus muon spin relaxation rate (σ_0, upper abscissa); black symbols: T_c versus planar oxygen quadrupole splitting $^{17}\nu_Q$ (lower abscissa). For list of abbreviations see Table 1. For triple layer Tl-2223 and Hg,Tl-1223 the pairs connected with a dotted line belong to the same sample and correspond to planar O sites of inner and outer layer (smaller splitting corresponds to underdoped inner CuO_2 layer). (**d**) T_c versus planar O hole density n_p calculated from $^{17}\nu_Q$ for all available data (see text). Black dotted lines are guides to the eye and connect different doping levels for one family. Solid grey line indicates increase of the maximum T_c (that is, for the optimal doping level) as a function of n_p. AF, antiferromagnetic; SC, superconducting phase.

cited therein. While trends relating the local charge distribution with T_c could be established, the uncertainty with regard to the EFG contributions from a variable CR chemistry, limited quantitative agreement with charge contents expected from stoichiometry, as well as insufficient experimental data hampered advances of such analyses.

Here we show that if we plot T_c versus the planar ^{17}O NMR quadrupole splitting, a functional dependence very similar to that of the Uemura plot emerges. This documents that the superfluid density is a function of the EFG at planar O. Based on very recent progress in the understanding of NMR quadrupole splittings in terms of the charge distribution in the CuO_2 plane[19] we show that the maximum T_c increases with the hole content of the planar O $2p_\sigma$ orbital, at the expense of that at Cu $3d_{x^2-y^2}$. Thus, we identify material chemistry parameters, the hole contents at planar Cu and O, that are largely temperature independent, yet determine the superfluid density at low temperatures. This finding stimulates the use of these orbital hole contents, calculated from NMR literature data[16,18–49], to draw a three-dimensional cuprate phase diagram that encompasses all cuprate families and has the superconducting domes ordered according to the maximum T_c. We argue that such a phase diagram might be very useful in discussing the complex properties of the cuprates.

Results

Superfluid density and charge densities in the CuO_2 plane. We plot in Fig. 1c, together with the original Uemura plot (in red), T_c versus $^{17}\nu_Q$ for similar materials and doping, and find a striking correspondence. This shows that the muon spin relaxation rate deep inside the superconducting state must be tied to the almost temperature independent EFG at the planar O nucleus, which determines the ^{17}O NMR splitting measured far above T_c, a rather unanticipated result.

It was confirmed recently, based on NMR data on the electron-doped and parent compounds, that NMR quadrupole splittings provide a quantitative measure of the charge distribution in the CuO_2 plane of apparently all cuprates[19]. A list of materials with abbreviations is given in Table 1. It was shown that the hole densities in the Cu $3d_{x^2-y^2}$ orbital (n_d) and the O $2p_\sigma$ orbital (n_p) in the CuO_2 plane are related to the experimentally measured splittings $^{63}\nu_Q$ at ^{63}Cu and $^{17}\nu_Q$ at ^{17}O as follows[18,19]:

$$^{17}\nu_Q = 2.45\,\mathrm{MHz}\cdot n_p + 0.39\,\mathrm{MHz}, \quad (1)$$

$$^{63}\nu_Q = 94.3\,\mathrm{MHz}\cdot n_d - 5.68\,\mathrm{MHz}\cdot\left(8-4n_p\right). \quad (2)$$

The planar oxygen splitting in equation (1) is only dependent on the hole content n_p of the onsite bonding orbital $2p_\sigma$ with the prefactor 2.45 MHz derived from the electric hyperfine interaction experimentally determined with atomic spectroscopy of the O $2p^5$ state[18]. The term of 0.39 MHz is due to the charge symmetry at planar oxygen in the ubiquitous CuO_2 plane, and this term is found to be rather independent on doping and similar for all families[19]. Therefore, one can easily convert the experimentally measured $^{17}\nu_Q$ into a reliable hole content n_p. The situation is somewhat more complicated for the Cu splitting in equation (2), which depends on the hole densities of both bonding orbitals. The first term is from the onsite hole content n_d of $3d_{x^2-y^2}$ with the prefactor 94.3 MHz, again derived from atomic spectroscopy of Cu $3d^9$ state[18]. The second term in equation (2) accounts for the EFG at the Cu nucleus caused by the charge in the bonding orbitals of the four surrounding planar O atoms, with the prefactor derived from the orbital overlap of O $2p_\sigma$ with the empty Cu $4p$ and the electric hyperfine interaction of the latter[18].

Table 1 | List of abbreviations.

Abbreviation	Formula
Bi-2212	$Bi_2Sr_2CaCu_2O_{8+\delta}$
CLBLCO_x	$(Ca_xLa_{1-x})(Ba_{1.75-x}La_{0.25+x})Cu_3O_{6+y}$
Hg-1201	$HgBa_2CuO_{4+\delta}$
Hg,Tl-1223	$Hg_{0.5}Tl_{0.5}Ba_2(Ca_{1-x}Sr_x)_2Cu_3O_{8+\delta}$
La-214	$La_{2-x}Sr_xCuO_4$
Nd-214	$Nd_{2-x}Ce_xCuO_4$
Pr-214	$Pr_{2-x}Ce_xCuO_4$
Tl-2201	$Tl_2Ba_2CuO_y$
Tl-2212	$Tl_2Ba_2CaCu_2O_{8-\delta}$
Tl-2223	$Tl_2Ba_2Ca_2Cu_3O_{10-\delta}$
Y-123	$YBa_2Cu_3O_{6+y}$
Y-124	$YBa_2Cu_4O_8$

First, we use equation (1) and convert all the planar oxygen splittings from the literature to n_p. The result is plotted in Fig. 1d, that is, we plot T_c versus n_p for the different materials. Of course, this plot is very similar to Fig. 1c, but it includes non-superconducting underdoped and parent materials with $T_c = 0$ K. We see that different cuprate families have rather different n_p, which results in the sorting of the families as in the Uemura plot. We also recognize that a large n_p is a prerequisite for a high maximum T_c, that is, at optimal doping. In Fig. 1d one can also notice a parabolic-like dependence of T_c on the oxygen charge n_p, which resembles the typical phase diagram that shows a dome-like dependence of T_c on the average doping level. The correlation between σ_0 and $^{17}\nu_Q$ is lost in the overdoped regime where σ_0 decreases with increasing doping[50,51], which was attributed to a decrease of n_s (ref. 52).

In Fig. 1d, we also included recent results for the electron-doped materials[19]. For $Nd_{1.85}Ce_{0.15}CuO_4$ the superfluid density was reported to be very similar to that of hole doped $YBa_2Cu_3O_{6+y}$, albeit measured optically and not by muon spin relaxation[3,53,54]. We find that these results are also in agreement with $^{17}\nu_Q$ splittings (see Supplementary Fig. 1) and corresponding hole contents for those two families, cf. Fig. 1d. Electron doping appears to be less efficient in providing a high T_c, but the rather high oxygen hole contents of the parent materials Pr_2CuO_4 and Nd_2CuO_4 suggest that hole doping should result in much higher T_c. The so-called infinite layer cuprate $Sr_{1-x}La_xCuO_2$, for which there are no reports of ^{17}O splittings, has the highest T_c among electron-doped families and a very high muon spin relaxation rate ($\sigma_0 \approx 4.5\,\mu s^{-1}$) (ref. 53), and we expect a high n_p. Indeed, a rather high T_c of more than 100 K was reported in the infinite layer system upon hole doping[55,56].

Clearly, a large n_p is a prerequisite for a high T_c, but is not sufficient, as expected for such a material chemistry parameter. If this empirical relation (max $T_c \propto n_p$) remains valid for higher oxygen hole content, the T_c of the cuprates might be raised substantially by the proper chemistry (we estimate 300–400 K per oxygen hole from the straight line in Fig. 1d).

The splittings of the ^{63}Cu NMR lines can only be converted into n_d if there are also ^{17}O NMR data available, cf. equation (2). However, there are much less ^{17}O splittings reported since the materials have to be enriched with ^{17}O (the naturally abundant ^{16}O nucleus has spin $I=0$) and therefore only part of ^{63}Cu splittings can be converted. (In Supplementary Fig. 1, we plot T_c versus experimentally measured splittings).

Note that the simple analysis using equations (1) and (2) gives hole densities that are in astonishingly good quantitative agreement with the total charge in the CuO_2 plane expected from the stoichiometry of the materials[19], that is,

$$1 + x = n_d + 2n_p, \quad (3)$$

where the factor of 2 accounts for the two O atoms per CuO_2.

This means that the sum of the hole contents n_d and n_p as determined with NMR (r.h.s.) equals the inherent Cu $3d^9$ hole content plus the hole content added by doping x (l.h.s.). This agreement was shown to apply for electron, as well as hole doping, and different parent materials differ only in terms of the charge transfer between Cu and O[19]. One can therefore also infer from Fig. 1d that compounds with the highest maximum T_c favour a smaller Cu hole content, and we conclude that it is the transfer of hole density to the O sites that is important for the highest T_c. With this result, one may ask if other properties of the cuprates should be discussed in terms of n_p and n_d, as well? This leads us to propose a cuprate phase diagram based on NMR.

Phase diagram of the cuprates based on NMR. In Fig. 2 we plot T_c as a function of n_d and $2n_p$ for all cuprates for which we could find both, Cu and O quadrupole splittings in the literature (see Supplementary Tables 1 and 2) with n_d and n_p calculated from equations (1) and (2). All materials appear in four separate groups, marked by colour: (1) $La_{2-x}Sr_xCuO_4$; (2) $YBa_2Cu_3O_{6+y}$, and other cuprates of that structure, for example, $(Ca_xLa_{1-x})(Ba_{1.75-x}La_{0.25+x})Cu_3O_{6+y}$ as well as $YBa_2Cu_4O_8$; (3) Bi, Tl and Hg based families; and finally, (4) the two electron-doped systems $Pr_{2-x}Ce_xCuO_4$ and $Nd_{2-x}Ce_xCuO_4$. The parent line, that is, the line that is given by $n_d+2n_p=1$ (bold dashed line) separates hole doped and electron-doped systems. Note that the lines parallel to the parent line are given by $n_d+2n_p=1+x$, and represent constant hole ($x=+0.1$, $+0.2$) or electron ($x=-0.1$, -0.2) doping. While there may be material-specific uncertainties, for example, La_2CuO_4 is not located exactly on the parent line, our straightforward analysis uncovers simple systematic trends concerning all cuprates, and we discuss some salient features now.

While n_d and n_p change significantly between different parent compounds along the line $n_d+2n_p=1$, antiferromagnetism persists as long as there is one hole per CuO_2. Such a large range of variation in the charge transfer in different parent compounds, with $2n_p$ ranging from 0.15 to 0.45, is perhaps quite surprising, and its further increase, if possible, could raise T_c substantially.

Doping holes means entering the right upper half of the $(2n_p, n_d)$-plane. While n_d and n_p increase with doping, the ratio of the respective changes $(\Delta n_d/2\Delta n_p)$ appears to be a family property, that is, parent materials with low n_p (for example, La_2CuO_4) add more holes to O than those with high n_p. With electron doping we enter the lower left half of the $(2n_p, n_d)$-plane. Here, predominantly Cu holes disappear while the (large) O hole content changes only slightly. It is not apparent from the phase diagram why most parent materials can only be doped with one type of carrier. As a function of doping, T_c increases with a slope that depends on the position on the parent line, as well, and hole doping seems to be more effective in raising T_c. Another important observation concerns optimal doping, that is, the doping level for which one finds the highest T_c for a given family. According to our analysis it is related to $x=n_d+2n_p-1$ and not particular values of n_d and n_p. However, we do observe a slight increase of the optimal x with increasing n_p (decreasing n_d). Note that the doping level x follows from our analysis in terms of n_d and n_p inserted into (3) and is not deduced from material chemistry. Our analysis agrees with expectations also for materials doped by interstitial O_δ where doping level x is often derived from the T_c dome[19]. Interestingly, the latter materials we find located in the same group, despite significant structural differences between Hg-, Tl- and Bi-based cuprates. Also the number of close CuO_2 layers in multi-layer systems does not result in significant differences in the charge distribution.

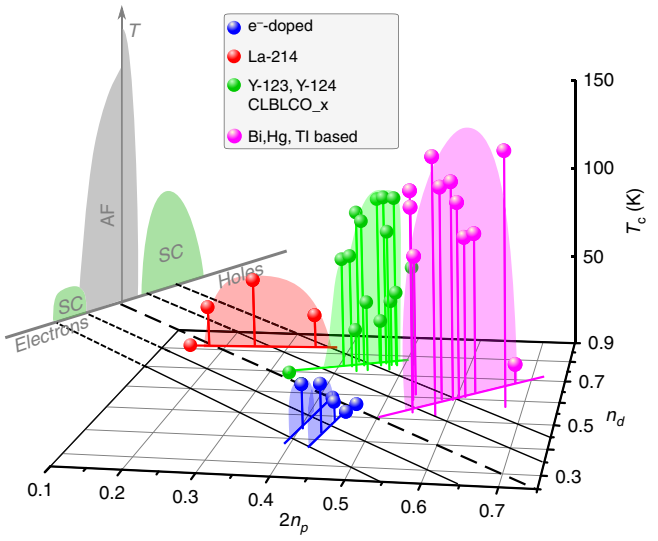

Figure 2 | Cuprate phase diagram from NMR. T_c as a function of oxygen ($2n_p$) and copper (n_d) hole content for hole doped La-214, Y-123, Y-124, CLBLCO_x and Bi-, Hg-, Tl-based compounds, as well as electron (e^-) doped Pr-214 and Nd-214. For list of abbreviations see Table 1. The parent line (dashed bold black) indicates expectation for the undoped case ($n_d+2n_p=1$ from $x=0$), parallel lines (thin black) correspond to expectation for doping $x=n_d+2n_p-1$ changing with a step of 0.1. The commonly used phase diagram (T versus x) appears as a projection (upper left).

Discussion

In Fig. 2 we plotted only T_c in the $(2n_p,n_d)$-phase diagram, but it might be of great interest to investigate whether other cuprate properties are better presented as a function of the local charge distribution, instead of the average doping level. While further analysis is beyond the scope of our paper, we shortly discuss some other cuprate properties with regard to our phase diagram.

The Néel temperature depends on the interlayer coupling and therefore is not expected to be dominated by the charge distribution in the CuO_2 plane. For example, $YBa_2Cu_3O_6$ has a higher T_N than Pr_2CuO_4 and La_2CuO_4. It would be interesting, however, to find out how the exchange coupling (J) changes along the parent line. Recently, there have been contradicting reports regarding J in the cuprates[57–59]. Mallet *et al.*[58] found no correlation between J and $T_{c,max}$ in $R(Ba, Sr)_2Cu_3O_y$, while Wulferding *et al.*[57] claimed that J is correlated with $T_{c,max}$ in $(Ca_xLa_{1-x})(Ba_{1.75-x}La_{0.25+x})Cu_3O_{6+y}$, which was later questioned by Tallon[59].

Structural parameters of the CuO_2 plane such as distances, buckling, or disorder appear to show no clear trend with respect to n_d and n_p. However, the apical oxygen distance from the CuO_2 plane increases as one follows the parent line beginning from low n_p, similar to the maximum possible T_c. This behaviour and the concomitant change in density of states of Cu 4*s* was noted before[60].

Pressure applied to underdoped cuprates usually increases T_c, while the structural changes to even hydrostatic pressure can be complicated[61]. For example, specifically strained $HgBa_2CuO_{4+\delta}$ can have almost identical CuO_6 octahedra as $La_{2-x}Sr_xCuO_4$, however, the large difference in their T_c values remains[62]. This might be related to the different values of n_d and n_p for these families. As a result of recent progress in anvil cell NMR[63,64], it is now possible to study cuprates at high pressures also with NMR[65], and it was found that the Cu splitting increases with pressure indicating changes in the planar hole contents[66].

However, single-crystal studies are necessary and ongoing efforts by our group aim at providing a quantitative measure of the local charge distribution as a function of pressure.

Another important issue concerns the heterogeneity of the cuprates. We know from NMR that the static charge and spin density can vary drastically within the CuO_2 plane, in particular between different cuprate families[67]. For example, the charge density in terms of the total doping x may easily vary by $\Delta x \approx 0.05$ (refs 32,68,69). Since T_c is not in a simple relation to this static inhomogeneity, only the average n_d and n_p appear to matter. From this, one would conclude that inhomogeneity is either not important for the maximum T_c, or it is ubiquitous and dynamically averaged for NMR, depending on the chemical environment.

To conclude, NMR measures the charge distribution in the bonding orbitals in the CuO_2 plane quantitatively, and since it reproduces the Uemura plot, that is, it finds the same ordering of families with respect to their maximum T_c, we now have material chemistry parameters that are responsible for setting the highest T_c and superfluid density. These findings inspired a different perspective on the cuprate phase diagram and it is likely that the complex cuprate properties might be better understood when discussed in the context of the charge distribution in the CuO_2 plane.

References

1. Uemura, Y. J. *et al.* Universal correlations between T_c and n_s/m^* (carrier density over effective mass) in high-T_c cuprate superconductors. *Phys. Rev. Lett.* **62,** 2317–2320 (1989).
2. Savici, A. T. *et al.* Muon spin relaxation studies of incommensurate magnetism and superconductivity in stage-4 $La_2CuO_{4.11}$ and $La_{1.88}Sr_{0.12}CuO_4$. *Phys. Rev. B* **66,** 014524 (2002).
3. Homes, C. C. *et al.* A universal scaling relation in high-temperature superconductors. *Nature* **430,** 539–541 (2004).
4. Tallon, J. L., Cooper, J. R., Naqib, S. H. & Loram, J. W. Scaling relation for the superfluid density of cuprate superconductors: origins and limits. *Phys. Rev. B* **73,** 180504 (2006).
5. Homes, C. C. Scaling of the superfluid density in strongly underdoped $YBa_2Cu_3O_{6+y}$: evidence for a Josephson phase. *Phys. Rev. B* **80,** 180509 (2009).
6. Dordevic, S. V., Basov, D. N. & Homes, C. C. Do organic and other exotic superconductors fail universal scaling relations? *Sci. Rep.* **3,** 1713 (2013).
7. Wu, D. *et al.* Superfluid density of $Ba(Fe_{1-x}M_x)_2As_2$ from optical experiments. *Phys. C Supercond.* **470,** S399–S400 (2010).
8. Homes, C. C., Xu, Z. J., Wen, J. S. & Gu, G. D. Effective medium approximation and the complex optical properties of the inhomogeneous superconductor $K_{0.8}Fe_{2-y}Se_2$. *Phys. Rev. B* **86,** 144530 (2012).
9. Shengelaya, A. & Müller, K. A. The intrinsic heterogeneity of superconductivity in the cuprates. *EPL* **109,** 27001 (2015).
10. Imry, Y., Strongin, M. & Homes, C. C. n_s - T_c correlations in granular superconductors. *Phys. Rev. Lett.* **109,** 067003 (2012).
11. Kogan, V. G. Homes scaling and BCS. *Phys. Rev. B* **87,** 220507 (R) (2013).
12. Lindner, M. H. & Auerbach, A. Conductivity of hard core bosons: a paradigm of a bad metal. *Phys. Rev. B* **81,** 054512 (2010).
13. Haase, J., Slichter, C. & Milling, C. Static charge and spin inhomogeneity in $La_{2-x}Sr_xCuO_4$ by NMR. *J. Supercond.* **15,** 339–343 (2002).
14. Ofer, R., Levy, S., Kanigel, A. & Keren, A. Charge-inhomogeneity doping relations in $YBa_2Cu_3O_y$ detected by angle-dependent nuclear quadrupole resonance. *Phys. Rev. B* **73,** 012503 (2006).
15. Schwarz, K., Ambrosch-Draxl, C. & Blaha, P. Charge distribution and electric-field gradients in $YBa_2Cu_3O_{7-x}$. *Phys. Rev. B* **42,** 2051–2061 (1990).
16. Zheng, G., Kitaoka, Y., Ishida, K. & Asayama, K. Local hole distribution in the CuO_2 plane of high-T_c Cu-oxides studied by Cu and oxygen NQR/NMR. *J. Phys. Soc. Jpn* **64,** 2524–2532 (1995).
17. Stoll, E. P., Meier, P. F. & Claxton, T. A. Electric field gradients from first-principles and point-ion calculations. *Phys. Rev. B* **65,** 064532 (2002).
18. Haase, J., Sushkov, O. P., Horsch, P. & Williams, G. Planar Cu and O hole densities in high-T_c cuprates determined with NMR. *Phys. Rev. B* **69,** 0945041 (2004).
19. Jurkutat, M. *et al.* Distribution of electrons and holes in cuprate superconductors as determined from ^{17}O and ^{63}Cu nuclear magnetic resonance. *Phys. Rev. B* **90,** 140504 (2014).
20. Ishida, K., Kitaoka, Y., Asayama, K., Kadowaki, K. & Mochiku, T. Cu NMR study in single crystal $Bi_2Sr_2CaCu_2O_8$ observation of gapless superconductivity. *J. Phys. Soc. Jpn* **63,** 1104–1113 (1994).
21. Fujiwara, K. *et al.* NMR and NQR studies of superconductivity in heavily doped $Tl_2Ba_2CuO_{6+y}$ with a single CuO_2 plane. *Phys. C Supercond.* **184,** 207–219 (1991).
22. Magishi, K. *et al.* Magnetic excitation and superconductivity in overdoped $TlSr_2CaCu_2O_{7-\delta}$: a ^{63}Cu NMR study. *Phys. Rev. B* **54,** 10131–10142 (1996).
23. Goto, T., Nakajima, S., Kikuchi, M., Syono, Y. & Fukase, T. $^{63/65}Cu$ and $^{203/205}Tl$ NMR study on the antiferromagnetic phase of the Tl-based high-T_c oxide $TlBa_2YCu_2O_7$. *Phys. Rev. B* **54,** 3562–3570 (1996).
24. Gerashenko, A. *et al.* The ^{63}Cu and ^{17}O NMR studies of spin susceptibility in differently doped $Tl_2Ba_2CaCu_2O_{8-\delta}$ compounds. *Phys. C. Supercond.* **328,** 163–176 (1999).
25. Han, Z. P., Dupree, R., Liu, R. & Edwards, P. ^{63}Cu NMR shift and relaxation behavior in $Tl_2Ba_2Ca_2Cu_3O_{10-\delta}$ ($T_c = 125$ K). *Phys. C. Supercond.* **226,** 106–112 (1994).
26. Williams, G. V. M., Krämer, S. & Mehring, M. Nuclear-quadrupole-resonance study of overdoped $Y_{1-x}Ca_xBa_2Cu_3O_7$. *Phys. Rev. B* **63,** 104514 (2001).
27. Zheng, G. *et al.* NMR study of local hole distribution, spin fluctuation and superconductivity in $Tl_2Ba_2Ca_2Cu_3O_{10}$. *Phys. C. Supercond.* **260,** 197–210 (1996).
28. Gippius, A. A., Antipov, E. V., Hoffmann, W. & Luders, K. Nuclear quadrupole interactions and charge localization in $HgBa_2CuO_{4+\delta}$ with different oxygen content. *Phys. C. Supercond.* **276,** 57–64 (1997).
29. Shimizu, S. *et al.* Planar CuO_2 hole density in high-T_c cuprates determined by NMR Knight shift: ^{63}Cu NMR on bilayered $Ba_2CaCu_2O_4(F,O)_2$ and three-layered $Ba_2Ca_2Cu_3O_6(F,O)_2$. *Phys. Rev. B* **83,** 144523 (2011).
30. Rybicki, D. *et al.* ^{63}Cu and ^{199}Hg NMR study of $HgBa_2CuO_{4+\delta}$ single crystals, Preprint at: http://arxiv.org/abs/1208.4690 (2012).
31. Keren, A., Kanigel, A. & Bazalitsky, G. Evidence for two fluids in cuprate superconductors from a nuclear resonance study of $(Ca_xLa_{1-x})(Ba_{1.75-x}La_{0.25+x})Cu_3O_y$. *Phys. Rev. B* **74,** 172506 (2006).
32. Rybicki, D. *et al.* Spatial inhomogeneities in single-crystal $HgBa_2CuO_{4+\delta}$ from ^{63}Cu NMR spin and quadrupole shifts. *J. Supercond. Nov. Magn.* **22,** 179–183 (2009).
33. Ohsugi, S., Tsuchiya, T., Koyama, T. & Fueki, K. Gapless superconductivity in overdoped Hg system; Cu-NQR study. *J. Low Temp. Phys.* **105,** 419–423 (1996).
34. Horvatić, M. *et al.* NMR investigation of $HgBa_2CaCu_2O_{6+\delta}$. *Phys. C. Supercond.* **235,** 1669–1670 (1994).
35. Julien, M.-H. *et al.* ^{63}Cu and ^{199}Hg NMR in overdoped $HgBa_2CaCu_2O_{6+\delta}$. *Phys. C. Supercond.* **268,** 197–204 (1996).
36. Julien, M.-H., Horvatić, M., Berthier, C. & Segransan, P. ^{63}Cu NMR in the normal state of $HgBa_2Ca_2Cu_3O_{8+\delta}$. *J. Low Temp. Phys.* **105,** 371–376 (1996).
37. Magishi, K. *et al.* ^{63}Cu NMR probe of superconducting properties in $HgBa_2Ca_2Cu_3O_{8+\delta}$: a possible reason for $T_c = 133$ K. *Phys. Rev. B* **53,** R8906–R8909 (1996).
38. Breitzke, H., Eremin, I., Manske, D., Antipov, E. & Luders, K. Formation of magnetic moments in the cuprate superconductor $Hg_{0.8}Cu_{0.2}Ba_2Ca_2Cu_3O_{8+\delta}$ below T_c seen by NQR. *Phys. C. Supercond.* **406,** 27–36 (2004).
39. Mikhalev, K. *et al.* ^{63}Cu NMR study of infinite-layer compound $Sr_{1-x}La_xCuO_2$. *Phys. C. Supercond.* **304,** 165–171 (1998).
40. Itohara, K. *et al.* Number of CuO_2 layers dependence of magnetic quantum criticality in homogeneously doped high-T_c copper oxides: a ^{63}Cu-NMR study on four-layered high- compounds $HgBa_2Ca_3Cu_4O_{8+y}$. *Phys. C. Supercond.* **470,** S140–S141 (2010).
41. Imai, T., Slichter, C., Cobb, J. & Markert, J. Superconductivity and spin fluctuations in the electron-doped infinitely-layered high T_c superconductor $Sr_{0.9}La_{0.1}CuO_2$ ($T_c = 42$ K). *J. Phys. Chem. Solids* **56,** 1921–1925 (1995).
42. Kotegawa, H. *et al.* Coexistence of superconductivity and antiferromagnetism in multilayered high-T_c superconductor $HgBa_2Ca_4Cu_5O_y$: Cu-NMR study. *Phys. Rev. B* **69,** 014501 (2004).
43. Mounce, A. M. *et al.* Absence of static loop-current magnetism at the apical oxygen site in $HgBa_2CuO_{4+\delta}$ from NMR. *Phys. Rev. Lett.* **111,** 187003 (2013).
44. Kambe, S., Yasuoka, H., Hayashi, A. & Ueda, Y. NMR study of the spin dynamics in $Tl_2Ba_2CuO_y$ ($T_c = 85$ K). *Phys. Rev. B* **47,** 2825–2834 (1993).
45. Takigawa, M. & Mitzi, D. B. NMR studies of spin excitations in superconducting $Bi_2Sr_2CaCu_2O_{8+\delta}$ single crystals. *Phys. Rev. Lett.* **73,** 1287–1290 (1994).
46. Crocker, J. *et al.* NMR studies of pseudogap and electronic inhomogeneity in $Bi_2Sr_2CaCu_2O_{8+\delta}$. *Phys. Rev. B* **84,** 224502 (2011).
47. Trokiner, A. *et al.* ^{17}O NMR in high-T_c superconductor $Tl_2Ba_2CaCu_2O_y$. *Phys. C. Supercond.* **255,** 204–210 (1995).
48. Lim, K., Lee, H. & Hur, N. An ^{17}O NMR study of $Hg_{0.5}Tl_{0.5}Ba_2(Ca_{1-x}Sr_x)_2Cu_3O_{8+\delta}$. *Phys. C. Supercond.* **232,** 215–221 (1994).
49. Amit, E. & Keren, A. Critical-doping universality for cuprate superconductors: Oxygen nuclear-magnetic-resonance investigation of $(Ca_xLa_{1-x})(Ba_{1.75-x}La_{0.25+x})Cu_3O_y$. *Phys. Rev. B* **82,** 172509 (2010).

50. Uemura, Y. J. *et al.* Magnetic-field penetration depth in $Tl_2Ba_2CuO_{6+\delta}$ in the overdoped regime. *Nature* **364,** 605–607 (1993).
51. Niedermayer, C. *et al.* Muon spin rotation study of the correlation between T_c and n_s/m^* in overdoped $Tl_2Ba_2CuO_{6+\delta}$. *Phys. Rev. Lett.* **71,** 1764–1767 (1993).
52. Tallon, J. L., Bernhard, C. & Niedermayer, C. Muon spin relaxation studies of superconducting cuprates. *Supercond. Sci. Technol.* **10,** A38–A51 (1997).
53. Shengelaya, A. *et al.* Muon-spin-rotation measurements of the penetration depth of the infinite-layer electron-doped $Sr_{0.9}La_{0.1}CuO_2$ cuprate superconductor. *Phys. Rev. Lett.* **94,** 127001 (2005).
54. Homes, C. C., Clayman, B. P., Peng, J. L. & Greene, R. L. Optical properties of $Nd_{1.85}Ce_{0.15}CuO_4$. *Phys. Rev. B* **56,** 5525–5534 (1997).
55. Azuma, M., Hiroi, Z., Takano, M., Bando, Y. & Takeda, Y. Superconductivity at 110 K in the infinite-layer compound $(Sr_{1-x}Ca_x)_{1-y}CuO_2$. *Nature* **356,** 775–776 (1992).
56. Chu, C., Deng, L. & Lv, B. Hole-doped cuprate high temperature superconductors. *Phys. C. Supercond.* **514,** 290–313 (2015).
57. Wulferding, D. *et al.* Relation between cuprate superconductivity and magnetism: a Raman study of $(CaLa)_1(BaLa)_2Cu_3O_y$. *Phys. Rev. B* **90,** 104511 (2014).
58. Mallett, B. P. P. *et al.* Dielectric versus magnetic pairing mechanisms in high-temperature cuprate superconductors investigated using Raman scattering. *Phys. Rev. Lett.* **111,** 237001 (2013).
59. Tallon, J. L. Anomalous behavior of T_c and pseudogap in the superconductor $Ca_xLa_{1-x}Ba_{1.75-x}La_{0.25+x}Cu_3O_y$ with respect to doping and ion size. *Phys. Rev. B* **90,** 214523 (2014).
60. Pavarini, E., Dasgupta, I., Saha-Dasgupta, T., Jepsen, O. & Andersen, O. K. Band-structure trend in hole-doped cuprates and correlation with $T_{c,max}$. *Phys. Rev. Lett.* **87,** 047003 (2001).
61. Schilling, J. S. in *High pressure effects in Handbook of High Temperature Superconductivity: Theory and Experiment* (eds Schrieffer, J. & Brooks, J.) (Springer Verlag, 2007).
62. Wang, S. *et al.* Strain derivatives of T_c in $HgBa_2CuO_{4+\delta}$: the CuO_2 plane alone is not enough. *Phys. Rev. B* **89,** 024515 (2014).
63. Haase, J., Goh, S. K., Meissner, T., Alireza, P. & Rybicki, D. High sensitivity nuclear magnetic resonance probe for anvil cell pressure experiments. *Rev. Sci. Intrum.* **80,** 073905 (2009).
64. Meissner, T. *et al.* New approach to high-pressure nuclear magnetic resonance with anvil cells. *J. Low Temp. Phys.* **159,** 284–287 (2010).
65. Meissner, T., Goh, S., Haase, J., Williams, G. V. M. & Littlewood, P. B. High-pressure spin shifts in the pseudogap regime of superconducting $YBa_2Cu_4O_8$ as revealed by ^{17}O NMR. *Phys. Rev. B* **83,** 220517 (2011).
66. Meissner, T. *Exploring nuclear magnetic resonance at the highest pressures - closing the pseudogap under pressure in a high temperature superconductor*. PhD thesis Univ. Leipzig (2012).
67. Haase, J. Charge density variation in $YBa_2Cu_3O_{6+y}$. *Phys. Rev. Lett.* **91,** 189701 (2003).
68. Jurkutat, M., Haase, J. & Erb, A. Charge inhomogeneity in electron-doped $Pr_{1.85}Ce_{0.15}CuO_4$ determined with ^{63}Cu NMR. *J. Supercond. Nov. Magn.* **26,** 2685–2688 (2013).
69. Singer, P. M., Hunt, A. W. & Imai, T. ^{63}Cu NQR evidence for spatial variation of hole concentration in $La_{2-x}Sr_xCuO_4$. *Phys. Rev. Lett.* **88,** 047602 (2002).

Acknowledgements

We are thankful to O.P. Sushkov, D. K. Morr, C.P. Slichter, G.V.M. Williams for helpful discussions, and acknowledge the financial support by the University of Leipzig, the DFG within the Graduate School Build-MoNa, the European Social Fund (ESF), the Free State of Saxony, and the Ministry of Science and Higher Education of Poland.

Author contributions

D.R., M.J. and S.R. contributed to data gathering, analysis and writing the manuscript. All the authors discussed the results and worked on the manuscript. C.K. helped with discussion of the μSR technique and its relation to NMR. J.H. supervised and contributed equally to the data analysis and manuscript editing, as well as providing project leadership.

Additional information

Supplementary Information accompanies this paper at http://www.nature.com/naturecommunications

Competing financial interests: The authors declare no competing financial interests.

Reprints and permission information is available online at http://npg.nature.com/reprintsandpermissions/

How to cite this article: Rybicki, D. *et al.* Perspective on the phase diagram of cuprate high-temperature superconductors. *Nat. Commun.* 7:11413 doi: 10.1038/ncomms11413 (2016).